PCCP

PAPER

View Article Online
View Journal | View Issue

Cite this: *Phys. Chem. Chem. Phys.*, 2023, **25**, 24819

Secondary ionization of pyrimidine nucleobases and their microhydrated derivatives in helium nanodroplets

Jakob D. Asmussen, [a] Abdul R. Abid,[a] Akgash Sundaralingam,[a] Björn Bastian,[a] Keshav Sishodia, [b] Subhendu De,[b] Ltaief Ben Ltaief, [a] Sivarama Krishnan,[b] Henrik B. Pedersen [a] and Marcel Mudrich *[a]

Radiation damage in biological systems by ionizing radiation is predominantly caused by secondary processes such as charge and energy transfer leading to the breaking of bonds in DNA. Here, we study the fragmentation of cytosine (Cyt) and thymine (Thy) molecules, clusters and microhydrated derivatives induced by direct and indirect ionization initiated by extreme-ultraviolet (XUV) irradiation. Photofragmentation mass spectra and photoelectron spectra of free Cyt and Thy molecules are compared with mass and electron spectra of Cyt/Thy clusters and microhydrated Cyt/Thy molecules formed by aggregation in superfluid helium (He) nanodroplets. Penning ionization after resonant excitation of the He droplets is generally found to cause less fragmentation compared to direct photoionization and charge-transfer ionization after photoionization of the He droplets. When Cyt/Thy molecules and oligomers are complexed with water molecules, their fragmentation is efficiently suppressed. However, a similar suppression of fragmentation is observed when homogeneous Cyt/Thy clusters are formed in He nanodroplets, indicating a general trend. Penning ionization electron spectra (PIES) of Cyt/Thy are broad and nearly featureless but PIES of their microhydrated derivatives point at a sequential ionization process ending in unfragmented microsolvated Cyt/Thy cations.

Received 21st June 2023,
Accepted 29th August 2023

DOI: 10.1039/d3cp02879h

rsc.li/pccp

1 Introduction

Ionization of deoxyribonucleic acid (DNA) bases is a key step in radiation damage leading to mutation.[1] Radiation damage is not only caused by direct impact of high-energy photons on the nucleobases, but to a large extent by secondary particles (electrons, ions and radicals) formed from reactions induced by the ionizing radiation.[2] The fragmentation of DNA bases upon ionization by collisions with electrons[3] and ions[4] has extensively been studied to unravel the key processes leading to radiation damage. An important element in understanding the reaction paths to damage of DNA is the interaction of the nucleobases with the aqueous medium which affects the ionization potential[5] and can alter the fragmentation pathways due to energy[6] or proton[7–9] transfer.

Fragmentation of molecular ions is readily studied in the gas phase using molecular beams techniques. Formation of microhydrated clusters (nucleobases weakly bound to a few water molecules) is possible in molecular beams, but controlling the cluster size is difficult.[10] In this study, we investigate the fragmentation of the two pyrimidine nucleobases cytosine (Cyt) and thymine (Thy) found in DNA (see Fig. 1) induced by direct and indirect ionization after XUV irradiation. Free Cyt and Thy molecules in an effusive beam are directly photoionized and Cyt/Thy clusters and microhydrated complexes are formed by means of aggregation in helium (He) nanodroplets (HNDs). HNDs are cold (0.4 K), superfluid clusters of weakly-bound He.[11] Due to their capability to efficiently pick up foreign species ('dopants'), the high mobility of dopants inside HNDs,

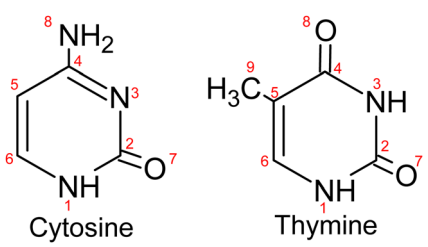

Fig. 1 Molecular structure of cytosine and thymine.

[a] Department of Physics and Astronomy, Aarhus University, 8000 Aarhus C, Denmark. E-mail: mudrich@phys.au.dk
[b] Quantum Center of Excellence for Diamond and Emergent Materials and Department of Physics, Indian Institute of Technology Madras, Chennai 600036, India

and their chemical inertness, various types of clusters can be formed and studied in HNDs. The size of the dopants' clusters is controlled by the partial pressure of the dopant vapor in the pick-up cell and can often be determined from a Poisson distribution.[12] In this way, we can achieve a relatively high degree of control of the composition of homogeneous and of heterogeneous clusters, such as microhydrated biomolecules. Dopants in HNDs can efficiently be Penning ionized through resonant excitation of the droplet, or through direct ionization of the droplet leading to radiative charge-transfer (RCT) ionization of the dopant.[13,14] Resonant photoexcitation is most efficient for the HND state excited at a photon energy $h\nu$ = 21.6 eV which correlates to the 1s2p ^{1}P atomic He state.[15] This state relaxes to the metastable 1s2s ^{1}S He atomic state within about 1 ps.[16,17] The metastable He atom further Penning ionizes the dopant by decaying to the ground state thereby releasing its energy to the dopant which in turn is ionized.[18] Penning ionization and RCT ionization are instances of indirect ionization processes in heterogeneous systems induced by energetic radiation, which have analogues in aqueous systems such as biological tissue.[19,20]

In this study, we aim at characterizing the fragmentation of Cyt and Thy by comparing direct photoionization of the free molecules in the gas-phase with indirect ionization of the molecules embedded in HNDs (see Fig. 2). By adjusting the doping level and by co-doping with water molecules, we measure fragment distributions from ionization of Thy and Cyt clusters and of the microhydrated Thy/Cyt molecules. As a general trend, fragmentation is efficiently suppressed when the molecules are complexed in clusters. From Penning ionization electron spectra (PIES) recorded in coincidence with various Thy/Cyt fragments and their complexes with water, we obtain some insight into the ionization process. Based on these results, we assess the benefit of HNDs as nano-matrices for studies of photoionization and fragmentation processes with relevance to radiation biology.

2 Methods

Ion mass spectra and electron velocity map images (VMIs) were measured using the XENIA (XUV electron–ion spectrometer for nanodroplets in Aarhus) endstation[21] located at the AMO-Line of the ASTRID2 synchrotron at Aarhus University, Denmark.[22] Using photoelectron–photoion coincidence (PEPICO) detection, VMIs were recorded in coincidence with specific fragment ions of Thy/Cyt molecules and clusters. Ion and electron yields were background-subtracted using a rotating chopper which periodically blocks and unblocks the HND beam. At the photon energy $h\nu$ = 21.6 eV (resonant excitation of HNDs), a tin (Sn) filter was used to block higher harmonics of the undulator radiation; at $h\nu$ = 26.0 eV (photoionization of HNDs), an aluminum (Al) filter was used. At the used experimental conditions (slit opening after the undulator and filters), a negligible contribution of higher-order radiation from the undulator is expected.[23] The relative photon flux is estimated from the yield of electron-H_2O^+ coincidences detected from the background gas.[24] Electron spectra were inferred from the VMI by Abel inversion using the MEVELER reconstruction method.[25]

HNDs were formed by continuous expansion of He at high pressure (30 bar) into vacuum through a cryogenically cooled (14 K) nozzle of diameter 5 μm. The average droplet size is determined from titration measurements to be $\langle N \rangle = 1.9 \times 10^4$.[26] The droplets were first doped with Cyt or Thy by passing them through a 1 cm long vapor cell. The cell was heated to 140–165 °C and 92–108 °C for doping with Cyt and Thy, respectively. The doping level for the two dopants is mainly determined from the monomer-to-dimer ratio detected at $h\nu$ = 21.6 eV for an oven temperature of 140 °C and 90 °C, respectively. Changes of the doping level from this value is then determined based on the change in vapor pressure as a function of varying oven temperature.[27] Subsequently, the HNDs were doped with H_2O or D_2O by leaking water vapor into a gas doping cell of length 1.8 cm further downstream. The doping level was determined using the formula derived by Kuma *et al.*[28] An effusive molecular beam of Cyt or Thy was realized by heating an effusive cell with a nozzle opening of 1 mm diameter. The cell was heated to 220 °C to create an effusive beam of Cyt and to 170 °C to create an effusive beam of Thy.

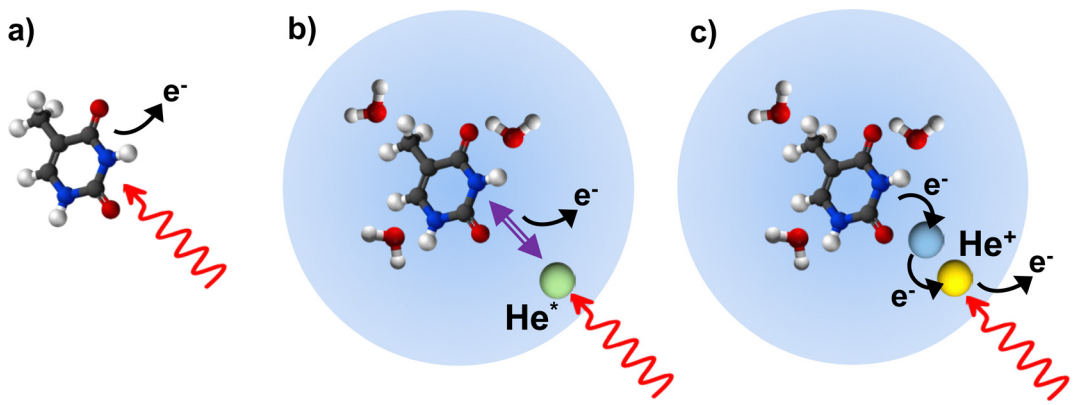

Fig. 2 Illustration of the three different ionization schemes for thymine and microhydrated thymine: (a) direct photoionization of the molecule, (b) Penning ionization in a helium nanodroplet following resonant excitation ($h\nu$ = 21.6 eV) of the droplet and (c) charge-transfer ionization in a helium nanodroplet after direct ionization of the droplet ($h\nu$ = 26 eV).

3 Results and discussion

3.1 Ion mass spectra

In Fig. 3, we present the ion mass spectra recorded by either photoionizing free Cyt and Thy molecules in an effusive beam or by indirectly ionizing Cyt and Thy embedded in HNDs at two photon energies $h\nu$ = 21.6 eV (Penning ionization) and $h\nu$ = 26 eV (RCT ionization). Additionally, mass spectra of microhydrated Cyt and Thy formed by co-doping the HNDs with Cyt/Thy and with D_2O molecules are shown (blue lines). Additionally, mass spectra of microhydrated Cyt and Thy formed by co-doping the HNDs with Cyt/Thy and with D_2O molecules are shown (blue lines). In the case of photoionization of the effusive beam, the photon energy is tuned to 20.6 eV and 24.6 eV; these values match the internal energy of the metastable He atom and the He ion which is released to the Cyt/Thy dopants by Penning ionization, respectively RCT ionization processes. We can estimate the probability for direct photoionization of the embedded dopant molecules relative to resonant excitation or ionization of the HND matrix at $h\nu$ = 21.6 eV and $h\nu$ = 26 eV by assuming one dopant per 104 He atoms. Comparing the photoionization cross-section for Thy (~100 Mb)[29] with that for resonant excitation (25 Mb)[13] and photoionization (6.79 Mb)[30] of He at the respective photon energies, we estimate a relative contribution of direct photoionization of Thy *vs.* secondary ionization to be $\lesssim$1% taking into account the efficiencies of Penning and RCT ionization.[31] Based on this estimate, we neglect contributions from direct photoionization of the embedded dopant in the case of Penning and RCT ionization. The photoionization cross-section of Cyt is unknown, but we expect it to be of the same order of magnitude as for Thy. In fact, previous attempts to detect dopants' photoelectrons and ions by directly photoionizing dopants in HNDs have remained unsuccessful except for a few particularly favorable cases.[32,33]

The various fragmentation channels of Cyt[34–36] and Thy[37–39] have been identified by means of high-resolution mass spectrometry and quantum chemical calculations. From photoionization of effusive Cyt and Thy, we identify two main fragments in agreement with mass spectra reported in the literature. The main fragmentation pathway of the parent cation involves the

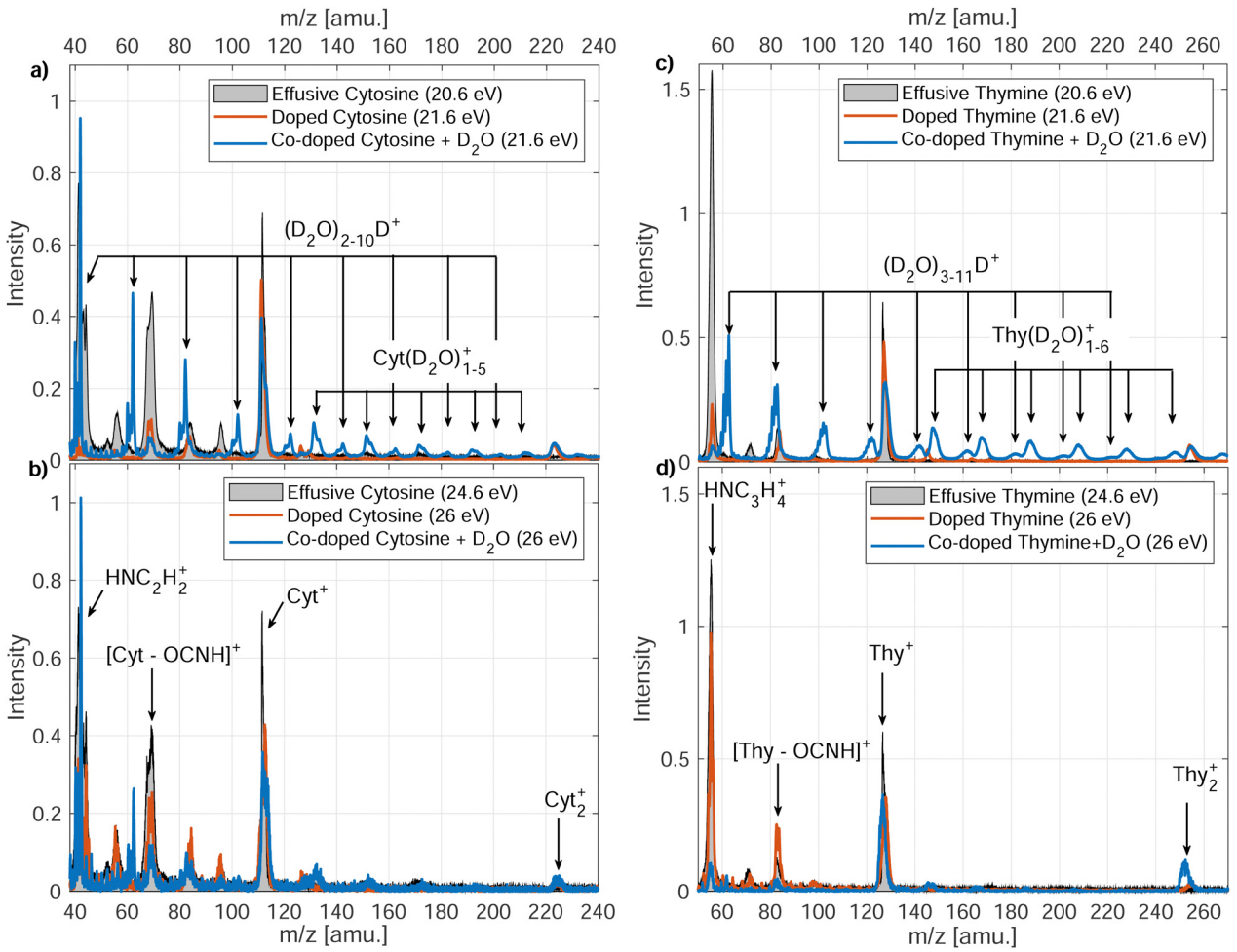

Fig. 3 Mass spectra recorded for Cyt [(a) and (b)] and Thy [(c) and (d)] in an effusive molecular beam, doped into HNDs or co-doped with D_2O into HNDs. (a) and (c) show the mass spectra for Penning ionization of the dopant ($h\nu$ = 21.6 eV), and (b) and (d) show mass spectra for charge-transfer ionization ($h\nu$ = 26 eV). In case of photoionization of the effusive beam, the photon energy is matched to the internal energy of the excited He atom inducing Penning ionization and to the He ion inducing charge-transfer ionization.

loss of isocyanic acid (OCNH) through a retro-Diels–Alder (rDA) reaction giving rise to the mass peaks at m/z = 68 and m/z = 83 for Cyt and Thy, respectively. The rDA reaction happens through breaking of the bonds N1–C2 and N3–C4 (see Fig. 1).[35,40] Both fragments are subjected to further fragmentation. The product of the rDA reaction of Cyt further fragments through the elimination of HCN (or NHC) as a result of break-up of the C5–C6 bond (or C4–C5).[35] This leads to the $HNC_2H_2^+$ fragment (m/z = 41). The Thy rDA product fragments through elimination of either CO or HCN (breaking of C4–C5 or C5–C6 bonds) resulting in fragments of masses m/z = 55 and m/z = 56.[40] Due to our limited mass resolution, we cannot fully separate the two ionic fragments in the effusive beam mass spectrum, but based on the center of joint mass peak, we identify CO elimination as the main pathway in consistence with previous findings.[37] Accordingly, the peak is identified as $HNC_3H_4^+$ (m/z = 55). In general, minor fragmentation paths leading to the aforementioned fragments with one or two missing or added hydrogen atoms are expected to be present but cannot be resolved with our spectrometer.

Indirect ionization of Cyt/Thy embedded in HNDs leads to similar fragments as direct photoionization of free Cyt/Thy. Additionally, we detect Cyt_2^+, Thy_2^+ clusters. We do not detect any fragments with masses between the monomer and dimer parent ions indicating that fragmentation of clusters in HNDs is limited to loss of intact parent moieties. In the case of RCT ionization ($h\nu$ = 26 eV), the relative yield of the fragments to the parent ion only slightly differs from that detected by photoionization of the effusive beam, whereas in the case of Penning ionization ($h\nu$ = 21.6 eV) the yield of the fragment ions are significantly suppressed. This shows that Penning ionization is a ''softer'' ionization channel where the excess energy is dissipated in the droplet thereby suppressing fragmentation. Penning ionization is generally a soft ionization channel for isolated species in the gas phase compared to other ionization mechanisms since the electron may carry away the excess energy.[41] Previous studies of electron-impact ionization of doped HNDs have reported reduced fragmentation of dopants in the droplet.[42–44] One study found that in particular fragmentation involving the break-up of C–C bonds was suppressed in HNDs[43] which matches well the observed reduction of the yields of fragments formed by HCN, NHC and CO elimination (relying on break-up of the C–C bonds) and increased yields of fragments from rDA (relying on break-up of N–C bonds).

Ions can efficiently be solvated in liquid He preventing them from being ejected from the HND.[45] The solvation efficiency may differ between different ion fragments, thus altering the relative yield between different ion species. However in a recent study, we found that the ion solvation has a minor effect on the RCT ion yield for the HND size used in this work.[31] For this reason, we expect ion solvation to only have a negligible impact on the detected ion yield.

In the case of microhydration of Cyt/Thy by co-doping with D_2O, the fragmentation of the pyrimidines is further suppressed. For Penning ionization, a series of D_2O cluster ions and Cyt/Thy ions with attached D_2O molecules can be seen in the mass spectra (see Fig. 4 for Penning ionization of microhydrated cytosine), whereas in the case of RCT ionization these cluster ions are less prominent. This further confirms the fact that Penning ionization is a softer ionization channel compared to RCT ionization. For the water cluster ions, the deuterated cluster, $(D_2O)_nD^+$, dominates over the undeuterated cluster, $(D_2O)_n^+$. Previous reports show that the unprotonated cluster is not observed for ionization of bare water clusters.[46,47] However, in HNDs the ejection of the OH, OD radical following proton-, respectively deuteron transfer can be inhibited.[48,49] For the microhydrated Cyt/Thy ion complex, the undeuterated cluster dominates over the deuterated cluster. Due to the high proton-affinity of the nucleobases,[50] one would expect the deuteron-transfer to be efficient towards Cyt/Thy. The fact that the undeuterated ion complexes have higher yields suggest that the ejection of the OH (OD) radical is less efficient for the mixed cluster. Denifl *et al.* have reported similar findings for ionization of HNDs co-doped with fullerene and water.[49]

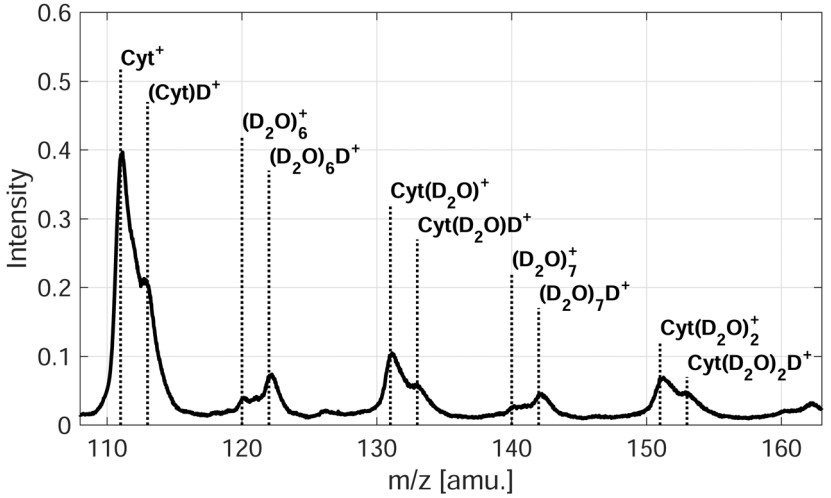

Fig. 4 Penning ionization mass spectrum ($h\nu$ = 21.6 eV) of microhydrated Cyt in He nanodroplets.

Fig. 5 (red symbols, right axis) shows the average size, $\langle n \rangle$, of the $Cyt(H_2O)_n^+$, $Thy(D_2O)_n^+$ ions detected as function of water doping level. Note that in the case of Cyt, we have replaced D_2O as co-dopant by H_2O as there was no particular advantage of using deuterated water. However, use of D_2O avoids the overlap in mass between the Thy parent ion and the $(H_2O)_7^+$ cluster. The average number of water molecules bound to the ionic complex rises with increasing doping level, but does not reflect the actual number of water molecules surrounding the Cyt/Thy molecule in the droplet since the average number of water molecules in the ionic complex is smaller than the average number of doped water molecules. We note that larger clusters ($n \geq 6$) may be present in mass spectra but are not considered here due to the limited resolution for larger masses. Thus, $\langle n \rangle$ shown in Fig. 5 is most likely underestimated; however it is unlikely that this explains the large difference (nearly factor 10) between the detected ion cluster size and the actual dopant cluster size. Thus, the microhydrated Cyt/Thy clusters fragment into smaller clusters (elimination of $[H_2O]_n/[D_2O]_n$) upon Penning and RCT ionization, where fragmentation is enhanced for RCT ionization as compared to Penning ionization. The rise of $\langle n \rangle$ seems to level out for high doping strength possibly indicating the presence of a hydration shell around the Cyt/Thy ion. A study of microhydrated Thy (and adenine) has shown a hydration shell of $n = 4$ around the nucleobase ion.[51] It would require higher doping levels to investigate whether convergence at $n = 4$ for the dopant ion is the case. However, we note that the $n = 4$ hydrated ion does not show an enhanced abundance compared to $n = 3$ and $n = 5$ in the mass spectra [Fig. 3(a) and (c)].

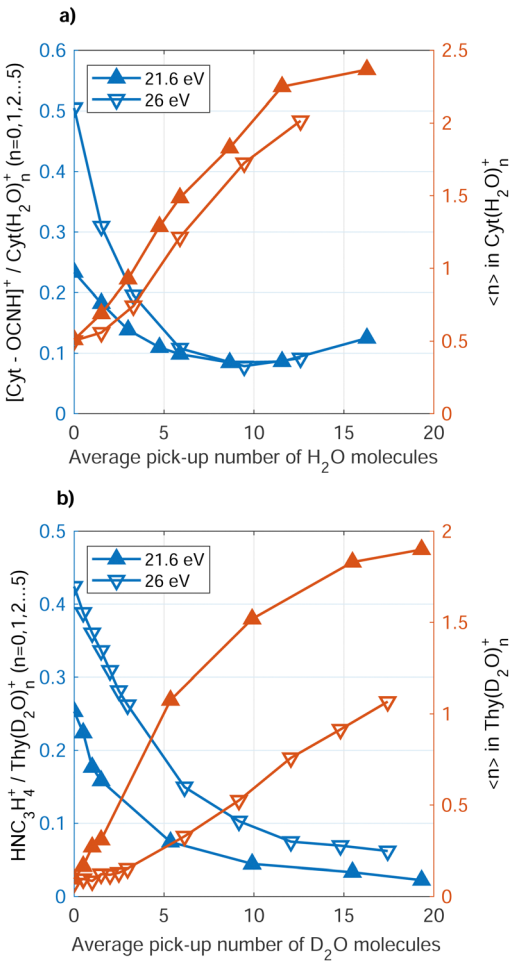

Fig. 5 Relative yields of $[Cyt-OCNH]^+$ to $Cyt(H_2O)_{0-5}^+$ (a) and of $NHC_3H_4^+$ to $Thy(D_2O)_{0-5}^+$ (b) as a function of H_2O/D_2O doping level (blue symbols, left axis). The red symbols and right axes show the average number of water molecules bound to the Cyt/Thy parent ions. For both dopants, the relative fragment yield and average number of attached water molecules are shown for Penning ionization ($h\nu$ = 21.6 eV) and charge-transfer ionization ($h\nu$ = 26 eV).

A clear trend is that the fragmentation of the Cyt/Thy molecules is suppressed by increasing the level of microhydration. Fig. 5 (blue symbols, left axis) shows the ratio of fragment ion $[Cyt-OCNH]^+$ ($NHC_3H_4^+$) to unfragmented ion $Cyt(H_2O)_{0-5}^+$ ($Thy[D_2O]_{0-5}^+$) yields for increasing doping level of water. We refer to the rDA product $[Cyt-OCNH]^+$ for Cyt and the product following CO elimination, $NHC_3H_4^+$, for Thy since the respective other main ion fragment of the two molecules overlap with a water cluster ion. Both for Penning ionization and RCT ionization, the ratio of fragment ions to hydrated and non-hydrated parent ion drops when increasing the number of added water molecules. In the case of Cyt, convergence of the ratio at 0.1 for both Penning and RCT ionization reflects the detection limit due to noise in the spectra.

Reduced fragmentation of glycine and tryptophan from RCT ionization in HNDs has been observed for increased level of co-doping level with water.[52,53] While microhydration clearly suppresses fragmentation of Cyt and Thy, naturally the question arises to what extend this "buffer effect" is a unique property of water. To answer this question, we performed comparative measurements where homogeneous Cyt/Thy clusters where formed in the HNDs. We measured the relative yield of the fragments to the parent ion and parent cluster ion for increased pure Cyt/Thy dopant clusters sizes. Fig. 6 shows the ratio of the yields of the two main fragments to total yield of the parent ions and parent ion clusters (Cyt_{1-4}^+, Thy_{1-4}^+) as a function of average dopant cluster size. The relative reduction in the dopant fragment ratio is 60–70% when increasing the average number of doped molecules from 0.5 to 2 in both cases of Penning and RCT ionization. A similar reduction of fragment yields with respect to monomers was observed for the case of impact ionization by keV ions.[54] In that study, new ion fragments were found for increasing Thy cluster sizes in a molecular beam which were facilitated by the intermolecular hydrogen-bonds in the cluster. These cluster-specific fragmentation channels are not present in HNDs most likely because conformations corresponding to local energy minima tend to be frozen out in HNDs at the expense of the equilibrium structures.[55,56]

The fact that the relative fragment yield decreases so rapidly for increasing pyrimidine cluster size without co-doping water indicates that the reduced fragmentation is a general trend for increasing cluster size largely independent of the molecular

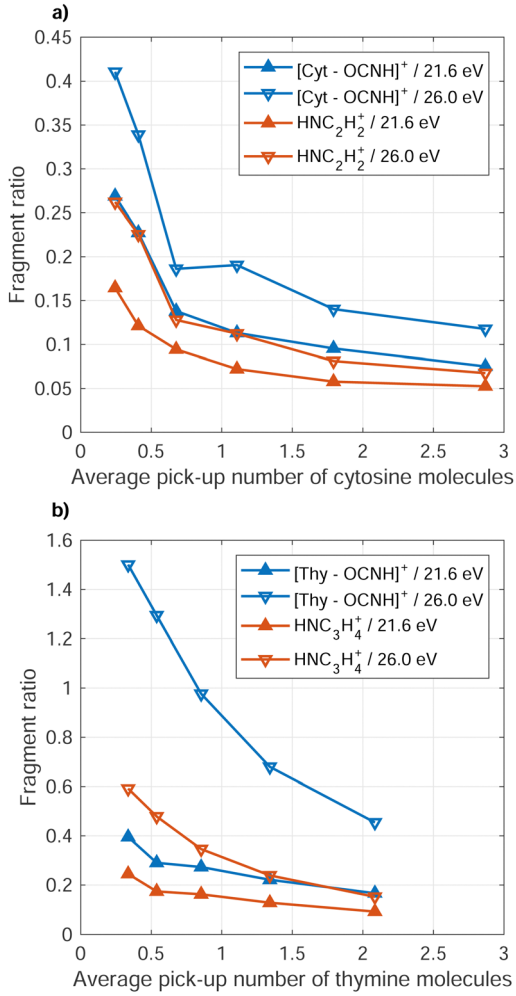

Fig. 6 Ratios of the yield of the two main fragments of Cyt (a) and Thy (b) to the sum of the parent ion and cluster yields (n = 1–4) for increasing doping level of Cyt/Thy. These data were obtained for Penning ionization ($h\nu$ = 21.6 eV) and charge-transfer ionization ($h\nu$ = 26 eV).

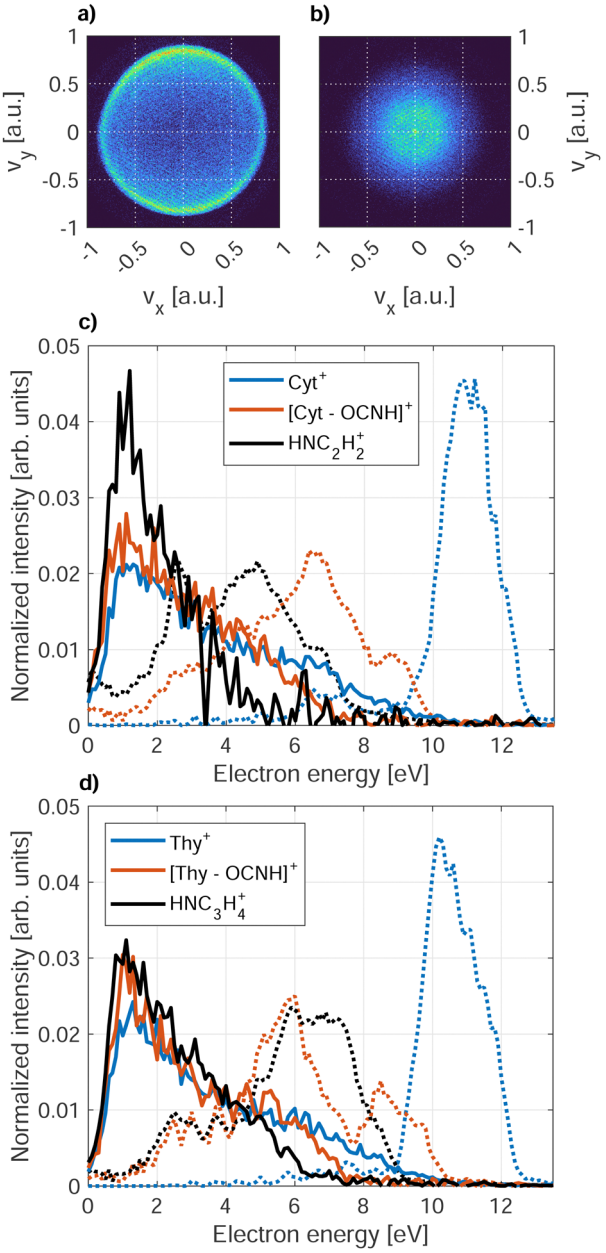

Fig. 7 VMIs of electrons in coincidence with Cyt^+ recorded for (a) direct photoionization of effusive Cyt ($h\nu$ = 20.6 eV) and (b) Penning ionization of Cyt in HNDs ($h\nu$ = 21.6 eV). Panels (c) and (d) show PIES ($h\nu$ = 21.6 eV) of HND-doped Cyt and Thy, respectively, for the three main electron–ion coincidence channels (solid lines). The dotted lines show the corresponding electron spectra of effusive Cyt and Thy ($h\nu$ = 20.6 eV).

composition. In the case of glycine and tryptophan in HNDs,[52,53] the degree to which fragmentation was buffered by water was different indicating dependencies on the intermolecular bonding in the dopant cluster. Thus, the buffering effect of fragmentation may be different for the purine bases (adenine and guanine) in HNDs and could possibly outcompete the buffering effect from formation of homogeneous purine clusters in the droplet. A systematic study of different combinations of co-dopants combined with quantum chemical calculations should be carried out to unravel the specific intermolecular effect of clusters on the suppression of fragmentation upon ionization.

3.2 Electron spectra

The PIES of dopants in HNDs are notoriously broad and structure-less.[33,57,58] An exception to this are alkali metals which reside on the droplet surface.[13,18,59] Fig. 7 shows PIES recorded at $h\nu$ = 21.6 eV and the corresponding PES recorded for an effusive beam at $h\nu$ = 20.6 eV in coincidence with the two main fragments and the parent ion for Cyt and Thy. The electron spectra recorded for effusive Cyt and Thy are consistent with those previously reported given the limited resolution of our VMI spectrometer.[40,60] The energy gap between the falling edges of the electron spectra for different coincidences towards larger kinetic energy matches the appearance energy of the different fragments reported for Thy.[40] In contrast, PIES of Cyt/Thy in HNDs are broad and structureless resembling previously reported PIES of polyatomic molecules embedded in

HNDs. The nature of the PIES in HNDs is still not well-described. We have previously modelled the PIES of acene molecules in HNDs by relaxation through a series of elastic electron-He binary collisions.[57] However, the droplet radius had to be overestimated by an order of magnitude to reach similar energy loss as observed in the experiment. We have recently demonstrated that the electron-He binary collision model can indeed reproduce the energy loss and change in angular distribution in the case of direct photoemission from pure HNDs.[61] Thus, our model is capable in describing energy loss which is solely due to elastic scattering, but we can confidently state that elastic scattering cannot alone account for the observed PIES. The sharp drop of signal at <1 eV was explained by the gap between the lower edge of the conduction band of liquid He and the vacuum level.[62–65] The falling edge of the PIES of acene molecules in HNDs could be modeled by a Maxwell–Boltzmann distribution corresponding to a thermal electron distribution with a temperature $>10^4$ K. However, this temperature is incompatible with the temperature of HNDs (0.4 K).[11] We note that such hot thermal emission of electrons has been described as ''hot electron ionization'' by Hansen *et al.*[66] for single-photon ionization,[67,68] multi-photon ionization[69,70] and Penning ionization[71] of fullerenes. If hot electron ionization were the main mechanism of electron emission by Penning ionization of Cyt/Thy in HNDs, it begs the question why it isn't in the case of direct photoionization of molecules in an effusive beam where mostly sharp peaks corresponding to discrete molecular orbitals are observed. Possibly, the presence of Cyt/Thy clusters in HNDs could cause changes of the electron spectra with respect to single molecules such as enhanced hot electron ionization; however at the doping conditions in the present experiment, mostly monomer doping is expected. Thus, there is presently little evidence for hot electron ionization as the cause of low-energy electron emission by Penning ionization of Cyt/Thy in HNDs. While the PIES tend to be dominated by a broad, low-energy electron distribution, rare gas atoms,[65] small organic molecules[58] and water (see Fig. 8) in HNDs do show additional better resolved, characteristic features in their PIES. Additional experimental and theoretical work is needed to unravel the dopant-specific mechanism of the Penning ionization process and the structure of the PIES in HNDs.

Fig. 8 shows the PIES recorded for microsolvated Cyt and Thy. The PIES recorded in coincidence with Cyt^+ or Thy^+ is identical in the case of doping only with the nucleobases and co-doping with water whereas the PIES detected in coincidence with $Cyt(H_2O)_{1-2}^+$ and $Thy(D_2O)_{1-2}^+$ extends to higher kinetic energy. This suggests that fragmentation of the microsolvated complex to the bare nucleobase ion is weak. Thus, the yields of Cyt^+ and Thy^+ mostly reflect Penning ionization in the case where no water molecules were captured by the droplet.

We note that the Penning ionization electron distribution extends to higher kinetic energy for the ion fragment associated to the smallest appearance energy. The difference in highest detected electron energy for the different fragments matches the difference in appearance energy which indicates that the

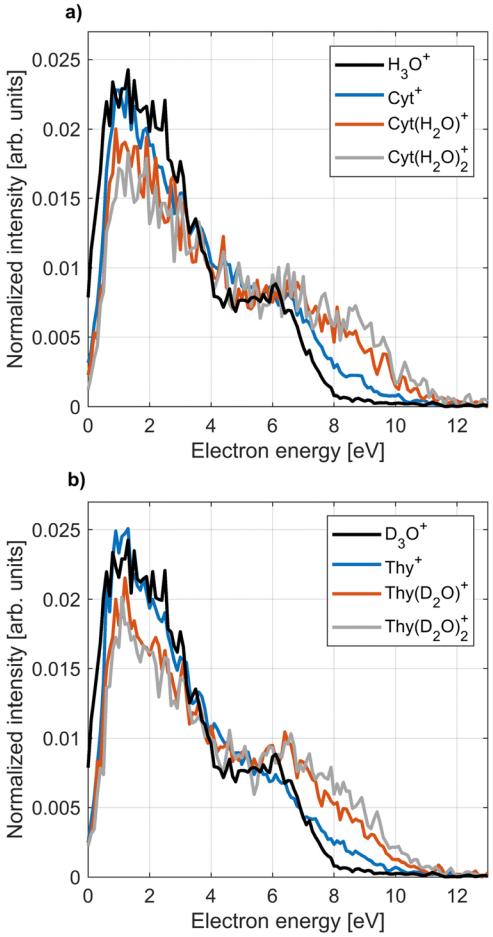

Fig. 8 PIES ($h\nu$ = 21.6 eV) of microsolvated Cyt (a) and Thy (b) in coincidence with the main water cluster ion fragment (H_3O^+/D_3O^+), the nucleobase parent ion and the ionic cluster of the parent ion bound to one or two water molecules.

Penning spectra can be associated to the appearance energy for a specific fragment of the dopant in HNDs. With this information, we can asses the PIES of microsolvated Cyt and Thy in Fig. 8. The PIES detected in coincidence with $Cyt(H_2O)_{1-2}^+$ and $Thy(D_2O)_{1-2}^+$ extend to higher kinetic energy than the PIES of Cyt^+, Thy^+ or H_3O^+/D_3O^+. Photoionization of hydrated nucleobases in a molecular beam expansion have revealed a red-shift of $\sim$0.3 eV in the appearance energy for $M(H_2O)_{1-2}^+$[72] which matches well with the observation of a more extended PIES in HNDs. The $Cyt(H_2O)_{1-2}^+/Thy(D_2O)_{1-2}^+$ shows a maximum in the PIES at $\sim$7 eV which is close to the maximum found in the PIES of H_3O^+/D_3O^+ ($\sim$6 eV). This indicates that the PIES of micro-hydrated dopants can be correlated to the PIES of water. This is expected, as the water molecules doped into the HNDs after the Cyt/Thy molecules form a hydration shell and Penning ionization is particularly surface-sensitive. Thus, despite their broad structure, the PIES give some insight into the secondary ionization of hydrated systems. However, more detailed understanding regarding the nature of the PIES of dopants is needed for any further analysis of the system.

4 Conclusion

In summary, we have presented mass spectra of Cyt and Thy and their microhydrated derivatives following Penning ionization and charge-transfer ionization in HNDs upon XUV irradiation. Fragmentation of the pyrimidine nucleobases is strongly suppressed upon ionization in helium nanodroplets compared to direct photoionization of the molecules in an effusive beam. Generally, the probability for the parent ion to fragment is smaller for Penning ionization making it a softer ionization process as compared to charge-transfer ionization. By increasing the dopant cluster size, either of the pure pyrimidine bases or by increasing the level of hydration of the pyrimidine molecules, fragmentation of the parent ion is also reduced for both ionization channels. The mass spectra of ionized Cyt and Thy clusters and microhydrated Cyt/Thy clusters in helium droplets deviate from clusters formed in a molecular beam expansion. The difference can most likely be assigned to the cold (0.4 K) environment of the helium droplets which facilitates stabilization of local minimum-energy structures.

Penning ionization electron spectra of Cyt/Thy and their microhydrated derivatives are broad and dissimilar to photoelectron spectra of effusive Cyt/Thy. Nevertheless, the highest kinetic energy of the Penning ionization electron spectra recorded in coincidence with ion fragments reflect the appearance energy of that fragment for direct photoionization.

These results demonstrate how a model system for radiation damage, *i.e.* microsolvated pyrimidine nucleobases, can be formed and studied in HNDs. Due to the efficient cooling of embedded species, helium droplets can give access to conformations not achievable under conventional molecular beams conditions. To obtain a more detailed understanding of the local minimum-energy conformations formed in HNDs and the quenching of fragmentation, further experiments and quantum chemistry calculations should be carried out.

Author contributions

J. D. A., A. R. A., A. S., B. B., K. S., S. D., L. B. L. and M. M. performed the experiments with support from H. B. P. S. K. aided remotely in the interpretation of the experimental results. J. D. A. and M. M. wrote the manuscript with input from all the co-authors.

Conflicts of interest

There are no conflicts to declare.

Acknowledgements

J. D. A. and M. M. acknowledge financial support by the Carlsberg Foundation. A. R. A. acknowledges with gratitude for the support from the Marie Skłodowska-Curie Postdoctoral Fellowship project Photochem-RS-RP (Grant Agreement No. 101068805) provided by the European Unions Horizon 2020 Research and Innovation Programme. S. R. K. thanks Dept. of Science and Technology, Govt. of India, for support through the DST-DAAD scheme and Science and Eng. Research Board. S. R. K., K. S., S. D. and M. M. acknowledge the support of the Scheme for Promotion of Academic Research Collaboration, Min. of Edu., Govt. of India, and the Institute of Excellence programme at IIT-Madras *via* the Quantum Center for Diamond and Emergent Materials. S. R. K. gratefully acknowledges support of the Max Planck Society's Partner group programme. S. R. K. acknowledges support for this research through the Indo-French Center for Promotion of Advanced Research (CEFIPRA). L. B. L. and M. M. acknowledge financial support by the Danish Council for Independent Research Fund (DFF) *via* Grant No. 1026-00299B. The research leading to this result has been supported by the COST Action CA21101 "Confined Molecular Systems: From a New Generation of Materials to the Stars (COSY)".

References

1 S. Steenken, *Chem. Rev.*, 1989, **89**, 503–520.
2 P. Swiderek, *Angew. Chem., Int. Ed.*, 2006, **45**, 4056–4059.
3 L. Sanche, *Eur. Phys. J. D*, 2005, **35**, 367–390.
4 M. Rodgers, S. Campbell, E. M. Marzluff and J. Beauchamp, *Int. J. Mass Spectrom. Ion Processes*, 1994, **137**, 121–149.
5 E. Cauët, M. Valiev and J. H. Weare, *J. Phys. Chem. B*, 2010, **114**, 5886–5894.
6 J. Kocisek, A. Pysanenko, M. Fárnk and J. Fedor, *J. Phys. Chem. Lett.*, 2016, **7**, 3401–3405.
7 K. Khistyaev, A. Golan, K. B. Bravaya, N. Orms, A. I. Krylov and M. Ahmed, *J. Phys. Chem. A*, 2013, **117**, 6789–6797.
8 D. Jacquemin, J. Zuniga, A. Requena and J. P. Céron-Carrasco, *Acc. Chem. Res.*, 2014, **47**, 2467–2474.
9 A. Semmeq, M. Badawi, A. Hasnaoui, S. Ouaskit and A. Monari, *Chem. – Eur. J.*, 2020, **26**, 11340–11344.
10 S. K. Kim, W. Lee and D. R. Herschbach, *J. Phys. Chem.*, 1996, **100**, 7933–7937.
11 J. P. Toennies and A. F. Vilesov, *Angew. Chem., Int. Ed.*, 2004, **43**, 2622–2648.
12 J. P. Toennies and A. F. Vilesov, *Annu. Rev. Phys. Chem.*, 1998, **49**, 1–41.
13 D. Buchta, S. R. Krishnan, N. B. Brauer, M. Drabbels, P. OKeeffe, M. Devetta, M. Di Fraia, C. Callegari, R. Richter and M. Coreno, *et al.*, *J. Phys. Chem. A*, 2013, **117**, 4394–4403.
14 J. H. Kim, D. S. Peterka, C. C. Wang and D. M. Neumark, *J. Chem. Phys.*, 2006, **124**, 214301.
15 M. Joppien, R. Karnbach and T. Möller, *Phys. Rev. Lett.*, 1993, **71**, 2654.
16 M. Mudrich, A. LaForge, A. Ciavardini, P. OKeeffe, C. Callegari, M. Coreno, A. Demidovich, M. Devetta, M. D. Fraia and M. Drabbels, *et al.*, *Nat. Commun.*, 2020, **11**, 112.
17 A. LaForge, J. Asmussen, B. Bastian, M. Bonanomi, C. Callegari, S. De, M. Di Fraia, L. Gorman, S. Hartweg and S. Krishnan, *et al.*, *Phys. Chem. Chem. Phys.*, 2022, **24**, 28844–28852.

18 L. Ben Ltaief, M. Shcherbinin, S. Mandal, S. Krishnan, A. LaForge, R. Richter, S. Turchini, N. Zema, T. Pfeifer and E. Fasshauer, *et al.*, *J. Phys. Chem. Lett.*, 2019, **10**, 6904–6909.
19 E. Alizadeh, T. M. Orlando and L. Sanche, *Annu. Rev. Phys. Chem.*, 2015, **66**, 379–398.
20 X. Ren, E. Wang, A. D. Skitnevskaya, A. B. Trofimov, K. Gokhberg and A. Dorn, *Nat. Phys.*, 2019, **14**, 1062–1066.
21 B. Bastian, J. D. Asmussen, L. Ben Ltaief, A. Czasch, N. C. Jones, S. V. Hoffmann, H. B. Pedersen and M. Mudrich, *Rev. Sci. Instrum.*, 2022, **93**, 075110.
22 N. Hertel and S. V. Hoffmann, *Synchrotron Radiat. News*, 2011, **24**, 19–23.
23 H. B. Pedersen, S. J. Lanng, B. Bastian, L. S. Harbo, S. V. Hoffmann, N. C. Jones, M. Mudrich, T. A. Nielsen, A. Svendsen and R. Teiwes, *Rev. Sci. Instrum.*, 2023, **94**, 053102.
24 G. Haddad and J. A. Samson, *J. Chem. Phys.*, 1986, **84**, 6623–6626.
25 B. Dick, *Phys. Chem. Chem. Phys.*, 2014, **16**, 570–580.
26 L. F. Gomez, E. Loginov, R. Sliter and A. F. Vilesov, *J. Chem. Phys.*, 2011, **135**, 154201.
27 D. Ferro, L. Bencivenni, R. Teghil and R. Mastromarino, *Thermochim. Acta*, 1980, **42**, 75–83.
28 S. Kuma, H. Goto, M. N. Slipchenko, A. F. Vilesov, A. Khramov and T. Momose, *J. Chem. Phys.*, 2007, **127**, 214301.
29 K. R. Koswattage, Y. Izumi and K. Nakagawa, *Quantum Beam Sci.*, 2020, **4**, 30.
30 J. Samson and W. C. Stolte, *J. Electron Spectrosc. Relat. Phenom.*, 2002, **123**, 265–276.
31 J. D. Asmussen, L. Ben Ltaief, K. Sishodia, A. R. Abid, B. Bastian, S. Krishnan, H. B. Pedersen and M. Mudrich, *J. Chem. Phys.*, 2023, **159**, 034301.
32 L. B. Ltaief, M. Shcherbinin, S. Mandal, S. R. Krishnan, R. Richter, T. Pfeifer and M. Mudrich, *J. Phys. B: At., Mol. Opt. Phys.*, 2020, **53**, 204001.
33 L. B. Ltaief, M. Shcherbinin, S. Mandal, S. Krishnan, R. Richter, S. Turchini, N. Zema and M. Mudrich, *J. Low Temp. Phys.*, 2021, **202**, 444–455.
34 O. Plekan, V. Feyer, R. Richter, M. Coreno, M. De Simone and K. Prince, *Chem. Phys.*, 2007, **334**, 53–63.
35 L. Sadr-Arani, P. Mignon, H. Chermette, H. Abdoul-Carime, B. Farizon and M. Farizon, *Phys. Chem. Chem. Phys.*, 2015, **17**, 11813–11826.
36 M. Shafranyosh, M. Zapotokova, M. Sukhoviya, V. Petrulyak and I. Shafranyosh, *Surf. Eng. Appl. Electrochem.*, 2022, **58**, 82–86.
37 M. Imhoff, Z. Deng and M. A. Huels, *Int. J. Mass Spectrom.*, 2005, **245**, 68–77.
38 P. J. van der Burgt, F. Mahon, G. Barrett and M. L. Gradziel, *Eur. Phys. J. D*, 2014, **68**, 1–9.
39 K. Majer, R. Signorell, M. F. Heringa, M. Goldmann, P. Hemberger and A. Bodi, *Chem. – Eur. J.*, 2019, **25**, 14192–14204.
40 H.-W. Jochims, M. Schwell, H. Baumgärtel and S. Leach, *Chem. Phys.*, 2005, **314**, 263–282.
41 D. Faubert, G. Paul, J. Giroux and M. Bertrand, *Int. J. Mass Spectrom. Ion Processes*, 1993, **124**, 69–77.
42 W. K. Lewis, B. E. Applegate, J. Sztáray, B. Sztáray, T. Baer, R. J. Bemish and R. E. Miller, *J. Am. Chem. Soc.*, 2004, **126**, 11283–11292.
43 S. Yang, S. M. Brereton, M. D. Wheeler and A. M. Ellis, *J. Phys. Chem. A*, 2006, **110**, 1791–1797.
44 S. Denifl, I. Mähr, F. Ferreira da Silva, F. Zappa, T. Märk and P. Scheier, *Eur. Phys. J. D*, 2009, **51**, 73–79.
45 K. Atkins, *Phys. Rev.*, 1959, **116**, 1339.
46 H. Shiromaru, H. Shinohara, N. Washida, H.-S. Yoo and K. Kimura, *Chem. Phys. Lett.*, 1987, **141**, 7–11.
47 R. T. Jongma, Y. Huang, S. Shi and A. M. Wodtke, *J. Phys. Chem. A*, 1998, **102**, 8847–8854.
48 S. Yang, S. M. Brereton, S. Nandhra, A. M. Ellis, B. Shang, L.-F. Yuan and J. Yang, *J. Chem. Phys.*, 2007, **127**, 134303.
49 S. Denifl, F. Zappa, I. Mähr, F. Ferreira da Silva, A. Aleem, A. Mauracher, M. Probst, J. Urban, P. Mach and A. Bacher, *et al.*, *Angew. Chem.*, 2009, **121**, 9102–9105.
50 M. Meot-Ner, *J. Am. Chem. Soc.*, 1979, **101**, 2396–2403.
51 N. J. Kim, Y. S. Kim, G. Jeong, T. K. Ahn and S. K. Kim, *Int. J. Mass Spectrom.*, 2002, **219**, 11–21.
52 Y. Ren, R. Moro and V. Kresin, *Eur. Phys. J. D*, 2007, **43**, 109–112.
53 Y. Ren and V. V. Kresin, *J. Chem. Phys.*, 2008, **128**, 074303.
54 T. Schlathölter, F. Alvarado, S. Bari, A. Lecointre, R. Hoekstra, V. Bernigaud, B. Manil, J. Rangama and B. Huber, *ChemPhysChem*, 2006, **7**, 2339–2345.
55 J. A. Davies, M. W. Hanson-Heine, N. A. Besley, A. Shirley, J. Trowers, S. Yang and A. M. Ellis, *Phys. Chem. Chem. Phys.*, 2019, **21**, 13950–13958.
56 D. Mani, N. Pal, M. Smialkowski, C. Beakovic, G. Schwaab and M. Havenith, *Phys. Chem. Chem. Phys.*, 2019, **21**, 20582–20587.
57 M. Shcherbinin, A. LaForge, M. Hanif, R. Richter and M. Mudrich, *J. Phys. Chem. A*, 2018, **122**, 1855–1860.
58 S. Mandal, R. Gopal, M. Shcherbinin, A. DElia, H. Srinivas, R. Richter, M. Coreno, B. Bapat, M. Mudrich and S. Krishnan, *et al.*, *Phys. Chem. Chem. Phys.*, 2020, **22**, 10149–10157.
59 J. D. Asmussen, R. Michiels, U. Bangert, N. Sisourat, M. Binz, L. Bruder, M. Danailov, M. Di Fraia, R. Feifel and L. Giannessi, *et al.*, *J. Phys. Chem. Lett.*, 2022, **13**, 4470–4478.
60 A. Trofimov, J. Schirmer, V. Kobychev, A. Potts, D. Holland and L. Karlsson, *J. Phys. B: At., Mol. Opt. Phys.*, 2005, **39**, 305.
61 J. D. Asmussen, K. Sishodia, B. Bastian, A. R. Abid, L. B. Ltaief, H. B. Pedersen, S. De, C. Medina, N. Pal and R. Richter, *et al.*, *Nanoscale*, 2023, **15**, 14025–14031.
62 M. Rosenblit and J. Jortner, *Phys. Rev. Lett.*, 1995, **75**, 4079.
63 U. Asaf and I. Steinberger, *Chem. Phys. Lett.*, 1986, **128**, 91–94.
64 H. Buchenau, J. Toennies and J. Northby, *J. Chem. Phys.*, 1991, **95**, 8134–8148.

65 C. C. Wang, O. Kornilov, O. Gessner, J. H. Kim, D. S. Peterka and D. M. Neumark, *J. Phys. Chem. A*, 2008, **112**, 9356–9365.
66 K. Hansen, *Statistical Physics of Nanoparticles in the Gas Phase*, 2018, pp. 331–348.
67 K. Hansen, R. Richter, M. Alagia, S. Stranges, L. Schio, P. Salén, V. Yatsyna, R. Feifel and V. Zhaunerchyk, *Phys. Rev. Lett.*, 2017, **118**, 103001.
68 Å. Andersson, L. Schio, R. Richter, M. Alagia, S. Stranges, P. Ferrari, K. Hansen and V. Zhaunerchyk, *Phys. Rev. A: At., Mol., Opt. Phys.*, 2023, **107**, 013103.
69 E. Campbell, K. Hansen, K. Hoffmann, G. Korn, M. Tchaplyguine, M. Wittmann and I. Hertel, *Phys. Rev. Lett.*, 2000, **84**, 2128.
70 M. Kjellberg, O. Johansson, F. Jonsson, A. Bulgakov, C. Bordas, E. E. Campbell and K. Hansen, *Phys. Rev. A: At., Mol., Opt. Phys.*, 2010, **81**, 023202.
71 J. Weber, K. Hansen, M.-W. Ruf and H. Hotop, *Chem. Phys.*, 1998, **239**, 271–286.
72 L. Belau, K. R. Wilson, S. R. Leone and M. Ahmed, *J. Phys. Chem. A*, 2007, **111**, 7562–7568.

